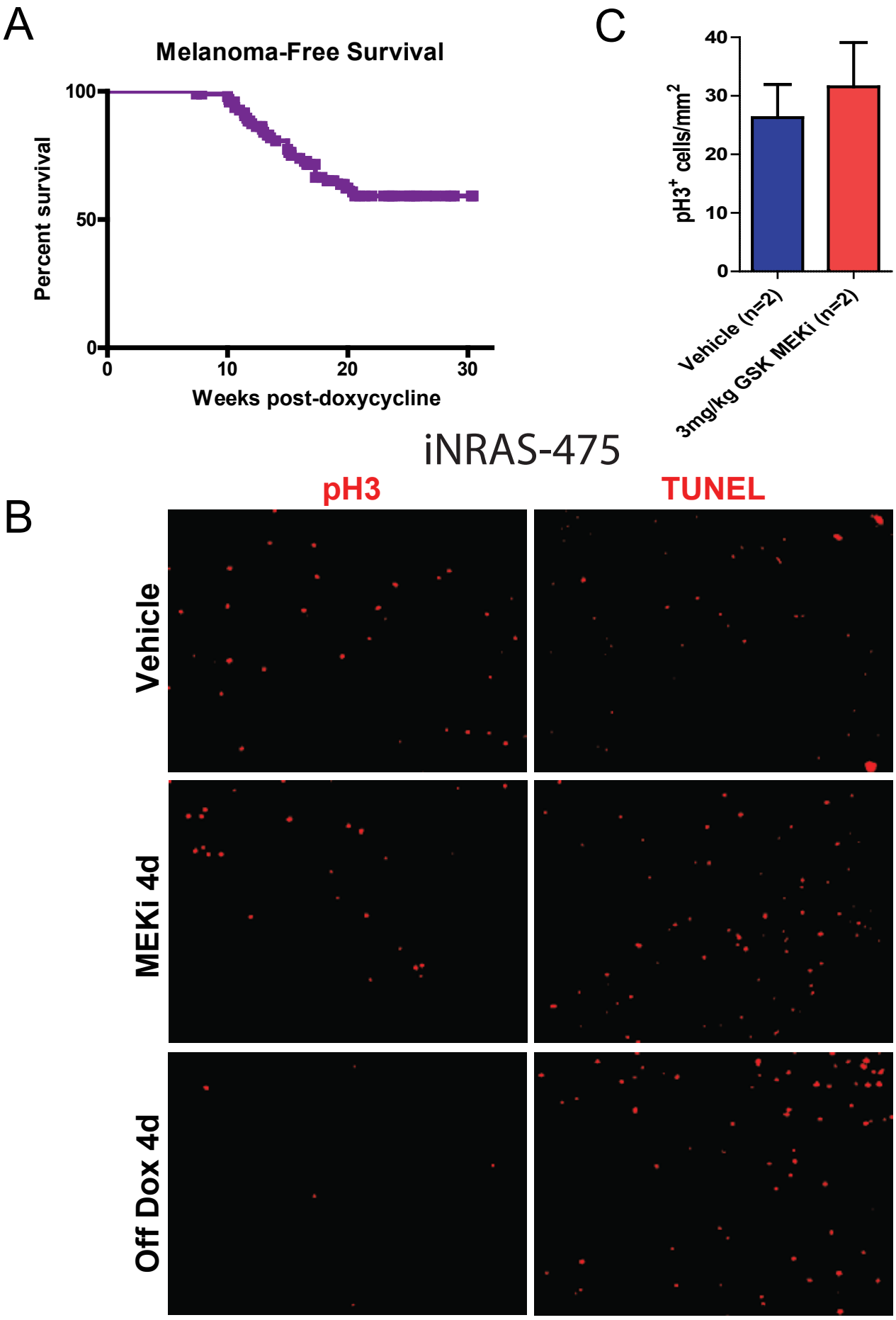

Supplementary Figure 1. Cellular proliferation is inhibited by NRAS extinction, but not MEK inhibition. (**a**) Kaplan-Meier curve depicting de novo melanoma-free survival in the iNRAS GEM model. (**b**) Staining and quantification for proliferation and apoptosis, as in Fig. 3a, from iNras-475 allografts. (**c**) Phospho-histone 3 quantification for iNras-475 tumors treated for four days with GSK1120212, 8 hours after the last dose.

Supplementary Figure 2. Pro-apoptotic mediators of MAPK inhibition are upregulated by both MEKi and NRAS extinction. The proapoptotic genes BIM and BMF are upregulated by both AZD6244 and NRAS extinction in iNRAS-475 tumors. (**a,b**) Microarray and (**c**) RPPA data are shown, n=6 each. Error bars are SEM.

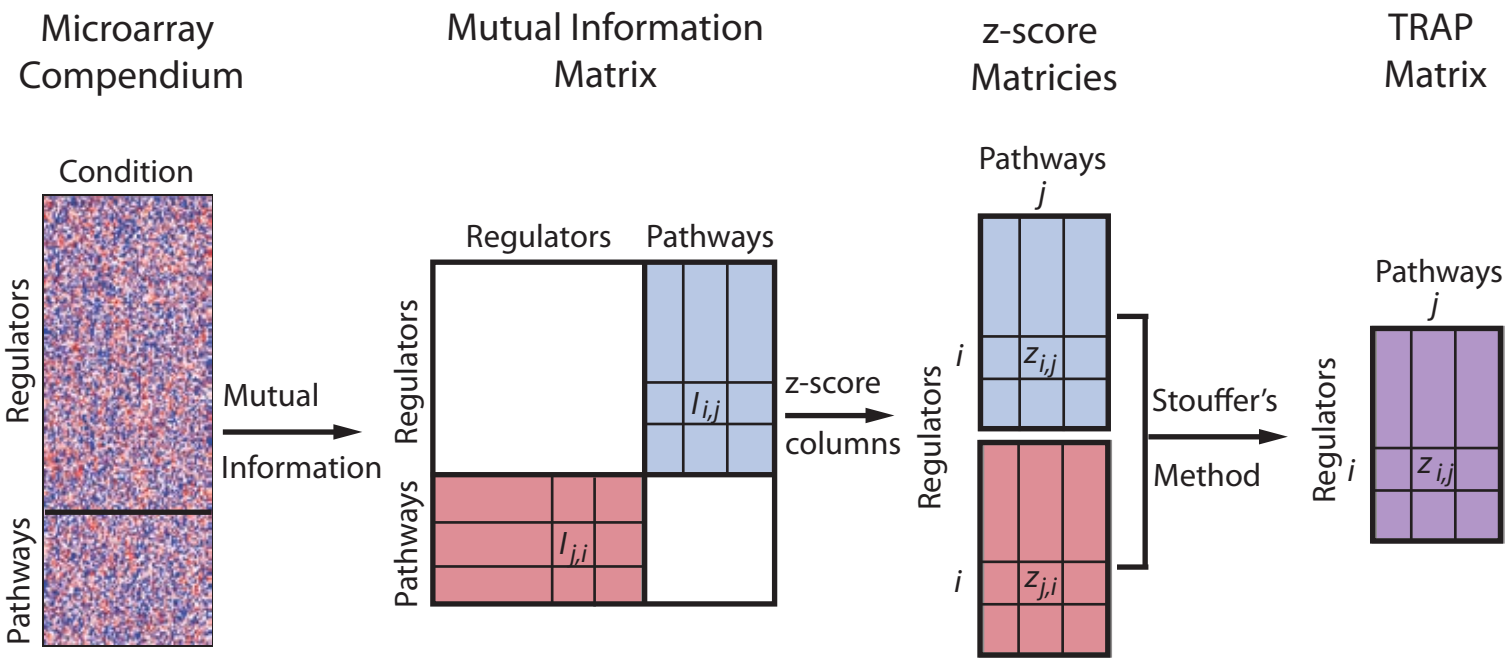

Supplementary Figure 3. TRAP network methodology. A full description of the method can be found in the Supplementary Methods. A compendium of over 3,000 mouse microarrays was compiled. Genes annotated as having transcriptional regulatory activity were separated from the genes that comprised canonical pathways. This matrix was used to calculate the mutual information between all regulators and pathways. Only connections between regulators and pathways were considered. The values were z-score transformed and combined using Stouffer's method to arrive at the final matrix of TRAP scores, which reflects the statistical significance of the relationship between any given transcriptional regulator and a canonical pathway.

A

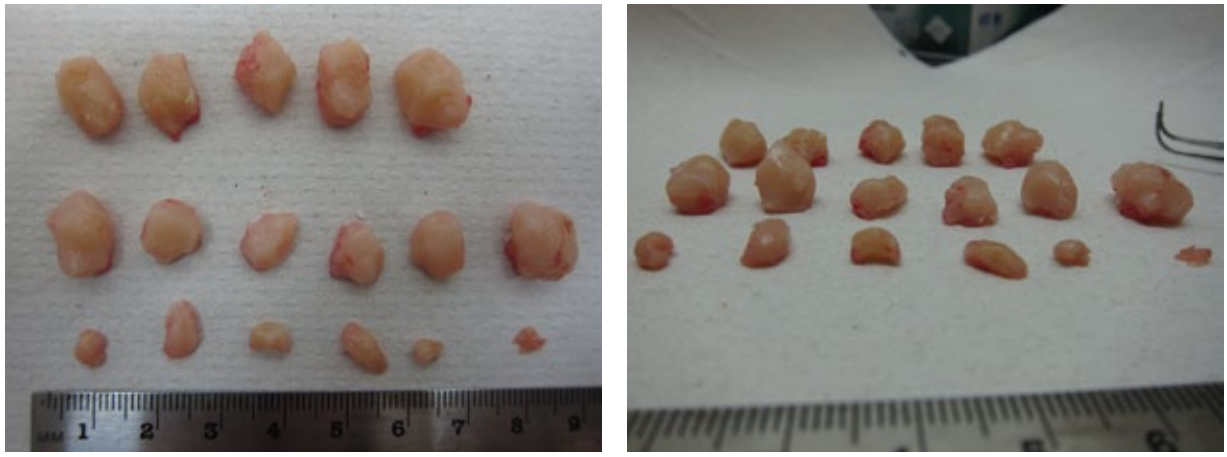

B

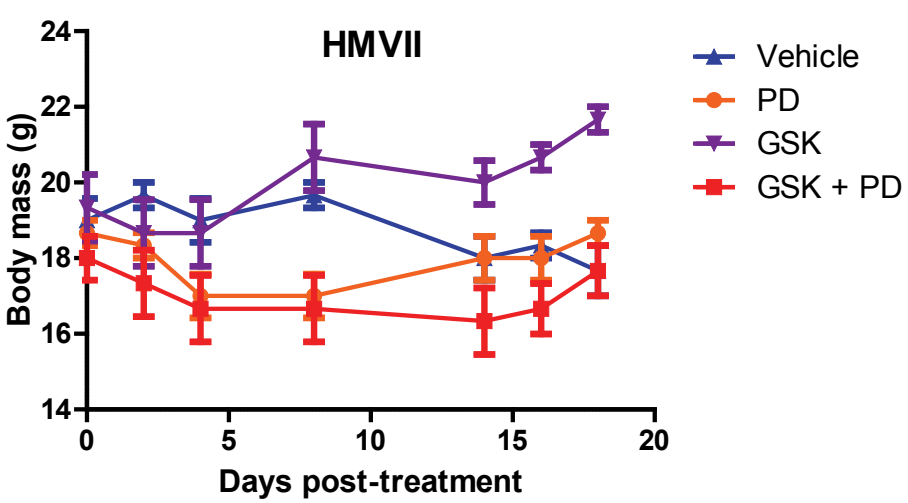

Supplementary Figure 4. Phenotypes of single and combined GSK1120212 and PD-0332991 treatment of NRAS-mutant melanomas. (**a**) iNRAS-475 tumors treated with single or combined doses of GSK1120212 and PD0332991, as depicted in Fig. 5b. Tumors were taken at the endpoint of 17 days post-dose. Vehicle controls were sacrificed earlier due to prohibitively large tumor mass and were not available for side-by-side comparison. The tumors are photographed from two angles to clearly show differences in height, in addition to length and width. (**b**) Body mass of the mice harboring HMVII tumors from Fig. 5c.

	p-val MEKi vs -NRAS d2	p-val MEKi vs -NRAS d4	MEKi avg	-NRAS d2 avg	-NRAS d4 avg
Rb-S807	**0.19**	**1.5E-09**	-0.19	**-0.04**	-0.88
Collagen VI	**0.03**	**1.2E-10**	0.26	**0.08**	0.85
Smad3	**0.9**	**2.1E-05**	-0.11	**-0.12**	-0.52
eIF4E	**8.7E-03**	**6.8E-06**	-0.03	**-0.15**	-0.18
IGF1Rb	**0.15**	**2.5E-06**	-0.16	**-0.27**	-0.69
Paxillin	**0.05**	**7.4E-07**	-0.05	**-0.21**	-0.57
p38 MAPK	**0.12**	**7.2E-05**	0.18	**0.07**	0.43
DJ-1	**0.09**	**1.4 E-03**	0.16	**0.04**	0.32
YBI	**0.17**	**2.3E-06**	-0.02	**0.05**	0.28
EGFR	**0.19**	**2.2E-04**	0.26	**0.14**	0.70

Supplementary Figure 5. RSM proteins in iNRAS-413 tumors after 2 days doxycycline withdrawal are not significantly differentially regulated compared to MEKi. Average RPPA measurements from 2 days doxycycline withdrawal (n=6) are compared to the values of the Top 10 RSM proteins in Fig. 4b. With only 2 exceptions (Collagen, eIF4E), 2 days off dox proteins are not significantly different from MEKi by a two-tailed student's t-test. Shown for comparison are p-values comparing MEKi to 4 days doxycycline withdrawal.